DISCRETE AND CONTINUOUS
DYNAMICAL SYSTEMS SERIES S
Volume **7**, Number **3**, June **2014**

doi:10.3934/xx.xx.xx.xx

pp. **X–XX**

# DISCUSSION ABOUT TRAFFIC JUNCTION MODELLING: CONSERVATION LAWS VS HAMILTON-JACOBI EQUATIONS

Guillaume Costeseque

Université Paris-Est, Ecole des Ponts ParisTech, CERMICS & IFSTTAR, GRETTIA
6 & 8 avenue Blaise Pascal, Cité Descartes, Champs sur Marne,
77455 Marne la Vallée Cedex 2, France.

Jean-Patrick Lebacque

Université Paris-Est, IFSTTAR, GRETTIA,
14-20 Boulevard Newton, Cité Descartes, Champs sur Marne,
77447 Marne la Vallée Cedex 2, France.

(Communicated by the associate editor name)

Abstract. In this paper, we consider a numerical scheme to solve first order Hamilton-Jacobi (HJ) equations posed on a junction. The main mathematical properties of the scheme are first recalled and then we give a traffic flow interpretation of the key elements. The scheme formulation is also adapted to compute the vehicles densities on a junction. The equivalent scheme for densities recovers the well-known Godunov scheme outside the junction point. We give two numerical illustrations for a merge and a diverge which are the two main types of traffic junctions. Some extensions to the junction model are finally discussed.

1. **Introduction.** There exist many mathematical methods to deal with road traffic modelling, including Hamilton-Jacobi (HJ) equations. However HJ theory has been mainly used up to now in the frame of an infinite one-directional road [7, 11, 29]. Hamilton-Jacobi equations have been introduced in [21] for modelling junction problems. The approach was very recently completed in [20]. To the best authors' knowledge, they are the only works which model the flow on a junction as a unique function. The works [17, 18] introduce also an Hamilton-Jacobi formulation for networks but they need to deal with tedious coupling conditions at each junction. Here the goal of this paper is to introduce a numerical scheme to solve the model from [21] and to give a traffic interpretation of this scheme. We mainly refer hereafter to [10] in which the mathematical properties of the numerical scheme have been deeply studied. Our scheme (10) is related to the Godunov scheme for conservation laws in one space dimension, as it is explained in our application to traffic in Section 3.

The outline of the paper is the following: in Section 2 we recall the main elements of the HJ model on junction and we introduce the numerical scheme for solving such equations. The main mathematical results from [10] are also recalled. In Section 3, we propose the traffic flow interpretation of our numerical results. In particular, the numerical scheme for HJ equations (10) is derived and the junction

2010 *Mathematics Subject Classification.* Primary: 65M06, 35F21; Secondary: 90B20.
*Key words and phrases.* Junction, numerical scheme, traffic, Hamilton-Jacobi equations.
The authors are supported by the ANR grant ANR-12-BS01-0008-01.

condition is interpreted in terms of traffic flow modelling. Indeed, we recover the well-known junction condition of Lebacque (see [25]) or equivalently those for the Riemann solver at the junction as in the book of Garavello and Piccoli [13]. Then in Section 4 we illustrate the numerical behaviour of our scheme for two cases of junctions: a diverge (one incoming and two outgoing branches) and a merge (two incoming and one outgoing branches) which are classical junction configurations for arterial traffic. Finally, we discuss some possible extensions for the HJ model in Section 5.

## 2. Hamilton-Jacobi framework.

### 2.1. Setting of the PDE problem.

In this subsection, we first define the junction, then the space of functions on the junction and finally the Hamilton-Jacobi Partial Differential Equation (HJ-PDE). We follow [21].

**The junction.** Let us consider $N \geq 1$ different unit vectors $e_\alpha \in \mathbb{R}^2$ for $\alpha = 1, \dots, N$. We define the branches as the half-lines generated by these unit vectors

$$J_\alpha = [0, +\infty) e_\alpha \quad \text{and} \quad J_\alpha^* = J_\alpha \setminus \{0\}, \quad \text{for all} \quad \alpha = 1, \dots, N,$$

and the whole *junction* (see Figure 1) as

$$J = \bigcup_{\alpha=1,\dots,N} J_\alpha.$$

The origin $y = 0$ is called the *junction point*. For a time $T > 0$, we also consider the time-space domain defined as

$$J_T = (0, T) \times J.$$

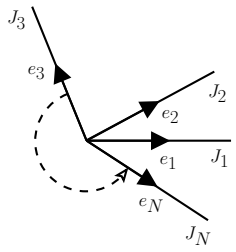


FIGURE 1. Junction model

**HJ equation on the junction.** We are interested in continuous functions $u : [0, T) \times J \to \mathbb{R}$ which are *viscosity solutions* (see Definition 3.3 in [10]) on $J_T$ of

$$\left\{ \begin{array}{l|l} u_t^\alpha + H_\alpha(u_x^\alpha) = 0 & \text{on} \quad (0,T) \times (0, +\infty), \quad \text{for} \quad \alpha = 1, \dots, N, \\ u^\beta =: \overline{u}, \quad \text{for all} \quad \beta = 1, \dots, N & \\ \overline{u}_t + \max\limits_{\beta=1,\dots,N} H_\beta^-(u_x^\beta) = 0 & \text{on} \quad (0,T) \times \{0\}, \end{array} \right. \tag{1}$$

for functions $H_\alpha$ and $H_\alpha^-$ that will be defined below in assumption (A1).

We consider an initial condition

$$u^\alpha(0,x) = u_0^\alpha(x), \quad \text{with} \quad x \in [0,+\infty) \quad \text{for} \quad \alpha = 1,\dots,N. \tag{2}$$

**Remark 1.** Following [21], we recall that (1) can be rigorously rewritten as

$$u_t + H(y,u_y) = 0, \quad \text{for} \quad (t,y) \in [0,T) \times J, \tag{3}$$

with

$$H(y,p) := \begin{cases} H_\alpha(p), & \text{for} \quad p \in \mathbb{R}, & \text{if} \quad y \in J_\alpha^*, \\ \max\limits_{\alpha=1,\dots,N} H_\alpha^-(p_\alpha), & \text{for} \quad p = (p_1,\dots,p_N) \in \mathbb{R}^{\mathbb{N}}, & \text{if} \quad y = 0, \end{cases}$$

subject to the initial condition

$$u(0,y) = u_0(y) := \left(u_0^\alpha(x)\right)_{\alpha=1,\dots,N}, \quad \text{for} \quad y = xe_\alpha \in J \quad \text{with} \quad x \in [0,+\infty). \tag{4}$$

This formulation highlights that HJ equation (3) subsumes all branches incident to the junction, making the state variable $u$ a vector. This approach is very new compared to what is done in traffic literature (see Subsection 3.3).

We make the following assumptions:

(A0) **Initial data**

The initial data $u_0 := (u_0^\alpha)_\alpha$ is globally Lipschitz continuous on $J$, i.e. each associated $u_0^\alpha$ is Lipschitz continuous on $[0,+\infty)$ and $u_0^\alpha(0) = u_0^\beta(0)$ for any $\alpha \neq \beta$.

(A1) **Strong convexity of the Hamiltonians**

We assume that there exists a constant $\gamma > 0$, such that for each $\alpha = 1,...,N$, there exists a lagrangian function $L_\alpha \in C^2(\mathbb{R};\mathbb{R})$ satisfying $L_\alpha'' \geq \gamma > 0$ such that $H_\alpha$ is the Legendre-Fenchel transform of $L_\alpha$ i.e.

$$H_\alpha(p) = L_\alpha^*(p) = \sup_{q\in\mathbb{R}} (pq - L_\alpha(q)). \tag{5}$$

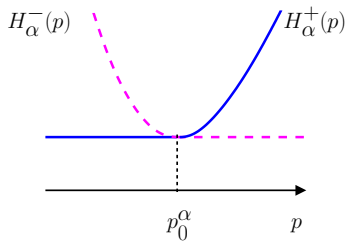


FIGURE 2. Illustration of Hamiltonian function

The assumption (A1) implies that

- the functions $H_\alpha \in C^1(\mathbb{R};\mathbb{R})$ are coercive, i.e. $\lim\limits_{|p|\to+\infty} H_\alpha(p) = +\infty$;

- and there exists a unique $p_0^\alpha \in \mathbb{R}$ such that $H_\alpha$ is non-increasing on $(-\infty, p_0^\alpha]$ and non-decreasing on $[p_0^\alpha, +\infty)$, and we set:

$$H_\alpha^-(p) = \begin{cases} H_\alpha(p) & \text{for} \quad p \leq p_0^\alpha \\ \\ H_\alpha(p_0^\alpha) & \text{for} \quad p \geq p_0^\alpha \end{cases}$$

and

$$H_\alpha^+(p) = \begin{cases} H_\alpha(p_0^\alpha) & \text{for} \quad p \leq p_0^\alpha \\ \\ H_\alpha(p) & \text{for} \quad p \geq p_0^\alpha \end{cases} \tag{6}$$

where $H_\alpha^-$ is non-increasing and $H_\alpha^+$ is non-decreasing (see Figure 2). Moreover, we have the following relationships

$$H_\alpha^-(p) = \sup_{q \leq 0} \left(pq - L_\alpha(q)\right) \quad \text{and} \quad H_\alpha^+(p) = \sup_{q \geq 0} \left(pq - L_\alpha(q)\right). \tag{7}$$

2.2. **Presentation of the scheme.** We denote by $\Delta x$ the space step and by $\Delta t$ the time step. We denote by $U_i^{\alpha,n}$ an approximation of $u^\alpha(n\Delta t, i\Delta x)$ for $n \in \mathbb{N},\ i \in \mathbb{N}$, where $\alpha$ stands for the index of the considered branch, as illustrated on Figure 3.

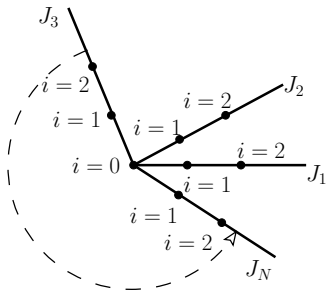


FIGURE 3. Discretization of the junction model

We define the discrete space derivatives

$$p_{i,+}^{\alpha,n} := \frac{U_{i+1}^{\alpha,n} - U_i^{\alpha,n}}{\Delta x} \quad \text{and} \quad p_{i,-}^{\alpha,n} := \frac{U_i^{\alpha,n} - U_{i-1}^{\alpha,n}}{\Delta x}, \tag{8}$$

and similarly the discrete time derivative

$$W_i^{\alpha,n} := \frac{U_i^{\alpha,n+1} - U_i^{\alpha,n}}{\Delta t}. \tag{9}$$

Then we consider the following numerical scheme corresponding to the discretization of the HJ equation (1) for $n \geq 0$:

$$\begin{cases} \dfrac{U_i^{\alpha,n+1} - U_i^{\alpha,n}}{\Delta t} + \max\left\{H_\alpha^+(p_{i,-}^{\alpha,n}), H_\alpha^-(p_{i,+}^{\alpha,n})\right\} = 0, & \text{for} \quad i \geq 1, \quad \alpha = 1, \dots, N, \\ U_0^{\beta,n} =: U_0^n, \quad \text{for all} \quad \beta = 1, \dots, N \\ \dfrac{U_0^{n+1} - U_0^n}{\Delta t} + \max\limits_{\beta=1,\dots,N} H_\beta^-(p_{0,+}^{\beta,n}) = 0 \end{cases} \Bigg| \quad \text{for} \quad i = 0, \tag{10}$$

with the initial condition

$$U_i^{\alpha,0} = u_0^\alpha(i\Delta x) \quad \text{for} \quad i \geq 1, \quad \alpha = 1, \dots, N. \tag{11}$$

As usual, it is natural to introduce a Courant-Friedrichs-Lewy (CFL) condition

$$\frac{\Delta x}{\Delta t} \geq \sup_{\substack{\alpha=1,\dots,N \\ p_\alpha \in [\underline{p}_\alpha, \overline{p}_\alpha]}} |H_\alpha'(p_\alpha)|. \tag{12}$$

It is easy to check that if the CFL condition (12) is satisfied, then the numerical scheme (10) is monotone.

2.3. **Main result: convergence of the numerical solution.** Hereafter is recalled one of the main results extracted from [10]. We particularly skip gradient and time derivatives estimates and also convergence property under weaker assumption than (A1) on the Hamiltonians. Interested readers are refered to [10].

Recall that under (A1), it is possible to recover the uniqueness of the solution (see [21]):

**Theorem 2.1. (Existence and uniqueness for a solution of the HJ-PDE)** *Assume (A0)-(A1) and let $T > 0$. Then there exists a unique viscosity solution $u$ of (1)-(2) on $J_T$ in the viscosity sense, satisfying for some constant $C_T > 0$*

$$|u(t,y) - u_0(y)| \leq C_T \quad \textit{for all} \quad (t,y) \in J_T.$$

*Moreover the function $u$ is Lipschitz continuous with respect to $(t,y)$ on $J_T$.*

Then from [10], we recover the following convergence result:

**Theorem 2.2. (Convergence of the numerical solution)** *Assume (A0)-(A1). Let $T > 0$ and $\varepsilon = (\Delta t, \Delta x)$ such that the CFL condition (12) is satisfied. If the function $u := (u^\alpha)_\alpha$ is the unique solution of (1)-(2) in the viscosity sense, then the numerical solution $(U_i^{\alpha,n})$ of (10)-(11) converges locally uniformly to $u$ when $\varepsilon \to 0$ on any compact set $\mathcal{K} \subset [0,T) \times J$, i.e.*

$$\limsup_{\varepsilon \to 0} \sup_{(n\Delta t, i\Delta x) \in \mathcal{K}} |u^\alpha(n\Delta t, i\Delta x) - U_i^{\alpha,n}| = 0 \tag{13}$$

*where the index $\alpha$ in (13) is chosen such that $(n\Delta t, i\Delta x) \in \mathcal{K} \cap [0,T) \times J_\alpha$.*

**Remark 2. (Extension to weaker assumptions on $H_\alpha$ than (A1))** All the results above can be extended if we consider some weaker conditions than (A1) on the Hamiltonians $H_\alpha$. Indeed, we can assume that $u_0$ and $H_\alpha$ for any $\alpha = 1, ..., N$ are at least locally Lipschitz. Such definitions are more accurate for our traffic application (see Section 3).

We need to consider that CFL condition (12) is replaced by the following one

$$\frac{\Delta x}{\Delta t} \geq \operatorname*{ess\,sup}_{\substack{\alpha=1,\dots,N \\ p_\alpha \in [\underline{p}_\alpha, \overline{p}_\alpha]}} |H'_\alpha(p_\alpha)|, \tag{14}$$

where ess sup denotes the essential supremum defined such as the smallest number $c$ for which the function $H'_\alpha$ only exceeds $c$ on a set of measure zero.

Using our scheme (10), we will present in Section 4 illustrations by numerical simulations with application to traffic.

## 3. Application to traffic flow.

As our motivation comes from traffic flow modelling, this section is devoted to the traffic interpretation of the model and the scheme. Notice that [21] has already focused on the meaning of the junction condition in this framework.

### 3.1. Settings.

We first recall the main variables adapted for road traffic modelling as they are already defined in [21]. We consider a junction with $N_I \geq 1$ incoming roads and $N_O \geq 1$ outgoing ones, such that $N_I + N_O =: N$.

**Densities and scalar conservation law.** We assume that the vehicles densities denoted by $(\rho^\alpha)_\alpha$ solve the following scalar conservation laws (also called LWR model for Lighthill, Whitham [28] and Richards [30]):

$$\begin{cases} \rho^\alpha_t + (f^\alpha(\rho^\alpha))_X = 0, & \text{for} \quad (t,X) \in [0,+\infty) \times (-\infty, 0), \quad \alpha = 1, ..., N_I, \\ \rho^\alpha_t + (f^\alpha(\rho^\alpha))_X = 0, & \text{for} \quad (t,X) \in [0,+\infty) \times (0, +\infty), \quad \alpha = N_I+1, ..., N_I+N_O, \end{cases} \tag{15}$$

where we assume that the junction point is located at the origin $X = 0$.

We assume that for any $\alpha$ the flux function $f^\alpha : \mathbb{R} \to \mathbb{R}$ reaches its unique maximum value for a critical density $\rho = \rho^\alpha_c > 0$ and it is non decreasing on $(-\infty, \rho^\alpha_c)$ and non-increasing on $(\rho^\alpha_c, +\infty)$. In traffic modelling, $\rho^\alpha \mapsto f^\alpha(\rho^\alpha)$ is usually called the *fundamental diagram*.

Let us define for any $\alpha = 1, ..., N$ the Demand function $f^\alpha_D$ (resp. the Supply function $f^\alpha_S$) such that

$$f^\alpha_D(p) = \begin{cases} f^\alpha(p) & \text{for} \quad p \leq \rho^\alpha_c \\ f^\alpha(\rho^\alpha_c) & \text{for} \quad p \geq \rho^\alpha_c \end{cases} \qquad \left( \text{resp.} \quad f^\alpha_S(p) = \begin{cases} f^\alpha(\rho^\alpha_c) & \text{for} \quad p \leq \rho^\alpha_c \\ f^\alpha(p) & \text{for} \quad p \geq \rho^\alpha_c \end{cases} \right). \tag{16}$$

These functions are illustrated on Figure 4.

We assume that we have a set of fixed coefficients $0 \leq (\gamma^\alpha)_\alpha \leq 1$ that denote:

- either the proportion of the flow from the branch $\alpha = 1, ..., N_I$ which enters in the junction,
- or the proportion of the flow on the branch $\alpha = N_I + 1, ..., N$ exiting from the junction.

We also assume the natural relations

$$\sum_{\alpha=1}^{N_I} \gamma^\alpha = 1 \quad \text{and} \quad \sum_{\beta=N_I+1}^{N_I+N_O} \gamma^\beta = 1.$$

**Remark 3.** We consider that the coefficients $(\gamma^\alpha)_{\alpha=1,...,N}$ are fixed and known at the beginning of the simulations. Such framework is particularly relevant for "quasi stationary" traffic flows.

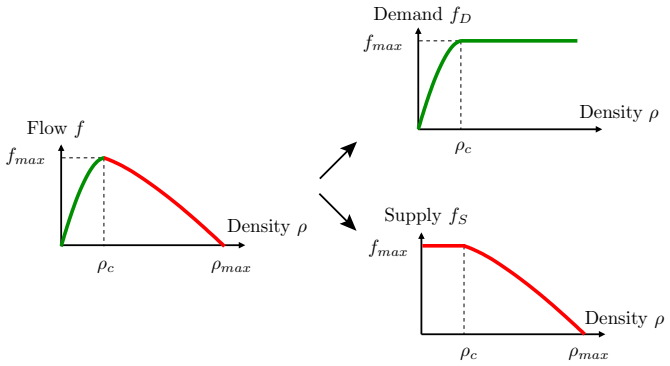


FIGURE 4. Supply and demand functions

**Vehicles labels and Hamilton-Jacobi equations.** Extending for any $N_I \geq 1$ the interpretation and the notations given in [21] for a single incoming road, let us consider the *continuous* analogue $u^\alpha$ of the discrete vehicles labels (in the present paper with labels increasing in the backward direction with respect to the flow)

$$\begin{cases} u^\alpha(t,x) = u(t,0) - \dfrac{1}{\gamma^\alpha}\displaystyle\int_0^{-x} \rho^\alpha(t,y)dy, & \text{for } x := -X > 0, \quad \text{if } \alpha \leq N_I, \\ \\ u^\beta(t,x) = u(t,0) - \dfrac{1}{\gamma^\beta}\displaystyle\int_0^{x} \rho^\beta(t,y)dy, & \text{for } x := X > 0, \quad \text{if } \beta \geq N_I + 1, \end{cases} \tag{17}$$

with equality of the functions at the junction point ($x = 0$), i.e.

$$u^\alpha(t,0) = u^\beta(t,0) =: u(t,0) \quad \text{for any} \quad \alpha, \beta. \tag{18}$$

where the common value $u(t,0)$ is nothing else than the (continuous) label of the vehicle at the junction point.

**Remark 4.** The vehicles labels are actually very useful for traffic management because on the one hand they are more reliable than flow and densities in-situ measurements and on the other hand, they give birth to the so-called Moskowitz function (or the Cumulative Vehicles Curves) of the labels on $(t,x)$ which is very tractable. See [23] for a complete review.

Following [21], for a suitable choice of the function $u(t,0)$, it is possible to check that the vehicles labels $u^\alpha$ satisfy the following Hamilton-Jacobi equation:

$$u_t^\alpha + H_\alpha(u_x^\alpha) = 0, \quad \text{for} \quad (t,x) \in [0,+\infty) \times (0,+\infty), \quad \alpha = 1, ..., N \tag{19}$$

where

$$H_\alpha(p) := \begin{cases} -\dfrac{1}{\gamma^\alpha} f^\alpha(\gamma^\alpha p) & \text{for} \quad \alpha = 1, ..., N_I, \\ \\ -\dfrac{1}{\gamma^\alpha} f^\alpha(-\gamma^\alpha p) & \text{for} \quad \alpha = N_I + 1, ..., N_I + N_O. \end{cases} \tag{20}$$

**Remark 5.** It worths to notice that the Hamiltonian $H_\alpha$ and the flow function $f^\alpha$ differ from a sign because flow function is classically assumed to be non-decreasing on $[0, \rho_c]$ and non-increasing on $[\rho_c, \rho_{max}]$ while it is the opposite for $H_\alpha$ according

to (A1). The convexity of $H_\alpha$ is a key element for the uniqueness of the HJ solution as it is explained in [21].

Following definitions of $H_\alpha^-$ and $H_\alpha^+$ in (6) we get

$$H_\alpha^-(p) = \begin{cases} -\dfrac{1}{\gamma^\alpha} f_D^\alpha(\gamma^\alpha p) & \text{for} \quad \alpha \leq N_I, \\ -\dfrac{1}{\gamma^\alpha} f_S^\alpha(-\gamma^\alpha p) & \text{for} \quad \alpha \geq N_I + 1, \end{cases}$$

and

$$H_\alpha^+(p) = \begin{cases} -\dfrac{1}{\gamma^\alpha} f_S^\alpha(\gamma^\alpha p) & \text{for} \quad \alpha \leq N_I, \\ -\dfrac{1}{\gamma^\alpha} f_D^\alpha(-\gamma^\alpha p) & \text{for} \quad \alpha \geq N_I + 1. \end{cases} \tag{21}$$

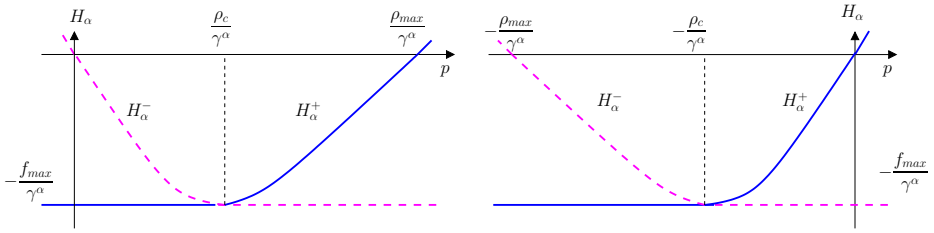


(a) Incoming branches (b) Outgoing branches

FIGURE 5. Graphs of the Hamiltonians

3.2. **Derived scheme for the densities.** The aim of this subsection is to properly express the numerical scheme satisfied by the densities in the traffic modelling framework. Let us recall that the density denoted by $\rho^\alpha$ is a solution of (15).

Let us consider a discretization with time step $\Delta t$ and space step $\Delta x$. Then we define the discrete car density $\rho_i^{\alpha,n} \geq 0$ for $n \geq 0$ and $i \in \mathbb{Z}$ (see Figure 6) by

$$\rho_i^{\alpha,n} := \begin{cases} \gamma^\alpha p_{|i|-1,+}^{\alpha,n}, & \text{for} \quad i \leq -1, \quad \alpha = 1, ..., N_I, \\ -\gamma^\alpha p_{i,+}^{\alpha,n}, & \text{for} \quad i \geq 0, \quad \alpha = N_I + 1, ..., N_I + N_O, \end{cases} \tag{22}$$

where we recall

$$p_{j,+}^{\alpha,n} := \frac{U_{j+1}^{\alpha,n} - U_j^{\alpha,n}}{\Delta x}, \quad \text{for} \quad j \in \mathbb{N}, \quad \alpha = 1, ..., N.$$

We have the following result:

**Lemma 3.1** (Derived numerical scheme for the density)**.**
*If $(U_i^{\alpha,n})$ stands for the solution of (10)-(11), then the density $(\rho_i^{\alpha,n})$ defined in (22)*

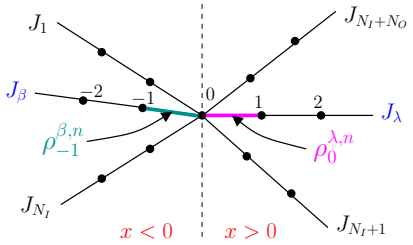


FIGURE 6. Discretization of the branches with the nodes for $(U_i^{\alpha,n})$ and the segments for $(\rho_i^{\alpha,n})$

*is a solution of the following numerical scheme for* $\alpha = 1, ..., N$

$$\frac{\Delta x}{\Delta t}\{\rho_i^{\alpha,n+1} - \rho_i^{\alpha,n}\} =$$

$$\begin{cases} F^\alpha(\rho_{i-1}^{\alpha,n}, \rho_i^{\alpha,n}) - F^\alpha(\rho_i^{\alpha,n}, \rho_{i+1}^{\alpha,n}) & \text{for } \begin{cases} i \le -1 & \text{if } \alpha \le N_I, \\ i \ge 1 & \text{else,} \end{cases} \\ F_0^\alpha\left((\rho_{-1}^{\beta,n})_{\beta\le N_I}, (\rho_0^{\lambda,n})_{\lambda \ge N_I+1}\right) - F^\alpha(\rho_i^{\alpha,n}, \rho_{i+1}^{\alpha,n}) & \text{for } i = 0, \quad \alpha \ge N_I + 1, \\ F^\alpha(\rho_{i-1}^{\alpha,n}, \rho_i^{\alpha,n}) - F_0^\alpha\left((\rho_{-1}^{\beta,n})_{\beta\le N_I}, (\rho_0^{\lambda,n})_{\lambda \ge N_I+1}\right) & \text{for } i = -1, \quad \alpha \le N_I, \end{cases} \tag{23}$$

*where we define the fluxes by*

$$\begin{cases} F^\alpha(\rho_{i-1}^{\alpha,n}, \rho_i^{\alpha,n}) := \min\left\{f_D^\alpha(\rho_{i-1}^{\alpha,n}),\ f_S^\alpha(\rho_i^{\alpha,n})\right\} & \text{for } \begin{cases} i \le -1 & \text{if } \alpha \le N_I, \\ i \ge 1 & \text{else,} \end{cases} \\ F_0^\alpha\left((\rho_{-1}^{\beta,n})_{\beta\le N_I}, (\rho_0^{\lambda,n})_{\lambda \ge N_I+1}\right) := \gamma^\alpha F_0 & \text{for } \alpha = 1, ..., N, \\ F_0 := \min\left\{\min_{\beta\le N_I} \frac{1}{\gamma^\beta} f_D^\beta(\rho_{-1}^{\beta,n}),\ \min_{\lambda\ge N_I+1} \frac{1}{\gamma^\lambda} f_S^\lambda(\rho_0^{\lambda,n})\right\}. \end{cases} \tag{24}$$

*and* $f_S^\alpha$, $f_D^\alpha$ *are defined in (16).*

*The initial condition is given by*

$$\rho_i^{\alpha,0} := \begin{cases} \gamma^\alpha \dfrac{u_0^\alpha(|i|\Delta x) - u_0^\alpha((|i|-1)\Delta x)}{\Delta x}, & \text{for } i \le -1, \quad \alpha \le N_I, \\ \gamma^\alpha \dfrac{u_0^\alpha(i\Delta x) - u_0^\alpha((i+1)\Delta x)}{\Delta x}, & \text{for } i \ge 0, \quad \alpha \ge N_I + 1. \end{cases} \tag{25}$$

The proof of Lemma 3.1 is available in [10].

**Remark 6.** Notice that (23) recovers the classical Godunov scheme [16] for $i \neq 0, -1$ while it is not standard for the two other cases $i = 0, -1$. Moreover we can check that independently of the chosen CFL condition, the scheme (23) is not monotone (at the junction, $i = 0$ or $i = -1$) if the total number of branches $N \ge 3$ and is monotone if $N = 2$ for a suitable CFL condition.

**Junction condition.** The junction condition in (1) reads

$$u_t(t,0) + \max_{\alpha=1,\dots,N} H_\alpha^-(u_x(t,0^+)) = 0. \tag{26}$$

It is a natural condition from the traffic point of view. Indeed condition (26) can be rewritten as

$$\begin{aligned} u_t(t,0) &= \sum_{1\le\alpha\le N_I} f^\alpha(\rho^\alpha(t,0^-)) \\ &= \min\left( \min_{\alpha=1,\dots,N_I} \frac{1}{\gamma^\alpha} f_D^\alpha(\rho^\alpha(t,0^-)), \min_{\beta=N_I+1,\dots,N} \frac{1}{\gamma^\beta} f_S^\beta(\rho^\beta(t,0^+)) \right). \end{aligned} \tag{27}$$

The condition (27) claims that the passing flux is equal to the minimum between the upstream demand and the downstream supply functions as they were presented by Lebacque in [25] (also for the case of junctions). This condition maximises the flow through the junction (also equal to the sum of all incoming flows or equivalently to the sum of all outgoing flows). Condition (27) could be recast as a linear optimization problem. Indeed if the densities $(\rho^\alpha(t,0^-))_{\alpha\le N_I}$ and $\left(\rho^\beta(t,0^+)\right)_{\beta\ge N_I+1}$ at the boundaries of the junction point are known at time $t \ge 0$, we then can compute the densities at time $t^+$ by solving

$$\begin{aligned} &\max \sum_{1\le\alpha\le N_I} f^\alpha(\rho^\alpha(t^+,0^-)) \\ &\text{s.t.} \left| \begin{array}{ll} 0 \le f^\alpha(\rho^\alpha(t^+,0^-) \le f_D^\alpha(\rho^\alpha(t,0^-)), & \forall \alpha \le N_I, \\ 0 \le f^\beta(\rho^\beta(t^+,0^+) \le f_S^\beta(\rho^\beta(t,0^+)), & \forall \beta \ge N_I+1, \\ 0 = f^\beta(\rho^\beta(t^+,0^+)) - \dfrac{\gamma^\beta}{\gamma^\alpha} f^\alpha(\rho^\alpha(t^+,0^-)), & \forall \alpha,\ \beta. \end{array} \right. \end{aligned} \tag{28}$$

where the constraints respectively express demand constraints on the incoming branches, supply constraints on outgoing branches and conservation of flows through the junction.

**Remark 7.** The supply and demand conditions in (28) prescribe the values of densities at the boundaries of the junction point. For instance, consider the demand constraint

$$f^\alpha(\rho^\alpha(t,0^-) \le f_D^\alpha(\rho^\alpha(t,0^-)), \quad \text{for any} \quad \alpha \le N_I. \tag{29}$$

We have to distinguish two cases:

- either there is equality in (29) and then the density at time $t^+$ is given by
$$\rho^\alpha(t^+,0^-) = (f_D^\alpha)^{-1}\left(f^\alpha(\rho^\alpha(t,0^-))\right),$$
- or we have the strict inequality in (29) and then the density at time $t^+$ becomes
$$\rho^\alpha(t^+,0^-) = (f_S^\alpha)^{-1}\left(f^\alpha(\rho^\alpha(t,0^-))\right).$$

3.3. **Review of the literature about junction modelling.** Junction modelling has recently attracted an increasing interest but it was considered a long time ago by traffic engineers. In first papers (see Chapters 8 and 9 of [14]) the approaches were mainly built on microscopic description of vehicles. In the present work we adopt a macroscopic point of view in which individual cars behaviors are not taken into account.

**Modelling approach.** Intersections models can be classified into two categories: pointwise models and spatial extended models. On the one hand, spatial

extended models consider the junction in its true space dimensions and analyze each conflicts between flows. These models offer a higher precision but also a greater complexity [24, 5]. On the other hand, pointwise models neglect the spatial dimension of the junction. Pointwise models are commonly restated in many instances as optimization problems [26, 27]. For sake of accuracy, some pointwise models take into account the node dynamics. The junction is seen as a buffer where incoming vehicles wait to be assigned on the outgoing roads. The literature often refers to internal state junction models [22]. The junction has an internal dynamics and it could be characterized by internal variables like the number of encompassed vehicles (denoted by $N$) or internal demand and supply constraints (respectively denoted by $\Delta(N)$ and $\Sigma(N)$ on Figure 7 (b)).

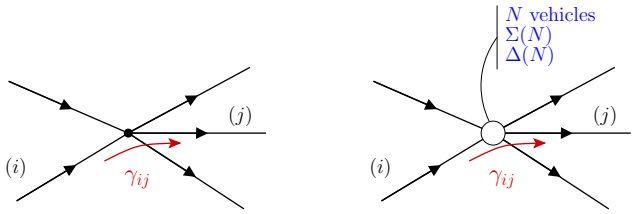


(a) Without internal dynamics (b) With internal dynamics

FIGURE 7. Pointwise junction models

Lebacque's works [26, 27] have shown that in case of vehicles equilibrium inside the junction (for which the time scale of internal dynamics is infinitely small in regard to the variation of upstream demand and downstream supply), internal state models and optimization pointwise models are strictly equivalent for merges (two incoming and one outgoing roads) and FIFO diverges (one incoming and two outgoing roads).

**General requirements.** Formalizing the ideas expressed in [22], the authors in [31] propose a list of seven generic requirements that should be verified by every first order macroscopic junction model:

- General applicability to any kind of junction, regardless to the number of incoming and outgoing roads: merge and diverge models which are not applicable for general junctions, are then totally excluded.
- Maximization of the flows from an user point of view: road users try to maximize their own velocity whenever it is possible. In practice each flow would increase until be restricted by some constraint. Then the through-flow is not necessarily the maximum possible according to the difference between system optimum and user optimum.
- Non-negativity of flows since traffic flow only propagates forward.
- Satisfaction of supply and demand constraints: the outflow from an incoming road (resp. the inflow into a outgoing road) can never exceed the demand (resp. the supply) at the boundary of the road.
- Conservation of vehicles: no vehicle appears or disappears at the junction.
- Conservation if turning fractions: the model has to consider the users route choices and it should not maximize the flows without considering the turning fractions of vehicles.

- Satisfaction of the invariance principle: stated first in [27] this principle expresses that the flows through the junction have to stay unchanged if the initial conditions (demand on incoming roads or supply on outgoing roads) are changed to the maximal capacity. Then (a) as long as a flow is limited by a capacity, a variation of its arriving demand cannot change the flow and (b) as long as a flow is not limited by a capacity, a variation of this capacity cannot change the flow.

In [12] and in [15], the authors consider an additional requirement:

- Internal supply constraints: such constraints are mainly justified for urban and regional junctions because they represent supply constraints due to vehicles interactions inside the junction. Such conflicts could be neglected for highways merges and diverges. However, [9] highlights that the uniqueness of the solution is not guaranteed with these additional constraints.

## 4. Simulations.

In this section, we present two numerical experiments. The main goal is to check if the numerical scheme (10)-(11) (or equivalently the scheme (23)-(25)) is able to illustrate the propagation of shock or rarefaction waves for densities through a junction. We propose to apply the scheme for some special configurations of junctions that is (i) a diverge for which the scheme was originally designed (see [21]) and (ii) a simple merge. The scheme has been also applied to a more complex junction in [10].

Notice that here the computations are carried out for the discrete variables $(U_i^{\alpha,n})$ while the densities $(\rho_i^{\alpha,n})$ are computed in a post-treatment using (22). It is also possible to compute directly the densities $(\rho_i^{\alpha,n})$ according to the numerical scheme (23).

### 4.1. Settings.

For the simulation, we consider that the flow functions are bi-parabolic (and only Lipschitz continuous) and defined as follows

$$f^\alpha(\rho) = \begin{cases} \dfrac{v^\alpha_{max}\rho^\alpha_c}{(\rho^\alpha_c)^2}\rho\left[(1-k)\rho + k\rho_{\max}\right], & \text{for} \quad \rho \leq \rho^\alpha_c, \\ \dfrac{v^\alpha_{max}\rho^\alpha_c}{(\rho^\alpha_{max}-\rho^\alpha_c)^2}[(1-k)\rho^2 + (k\rho^\alpha_c + (k-2)\rho^\alpha_{max})\rho & \\ \qquad -\rho^\alpha_{max}(k\rho^\alpha_c - \rho^\alpha_{max})], & \text{for} \quad \rho > \rho^\alpha_c, \end{cases}$$

where $k = 1.5$. The jam density $\rho^\alpha_c$ (resp. the maximal density $\rho^\alpha_{max}$) on branch $\alpha$ is obtained as the product of the nominal jam density $\rho_c = 20\ veh/km$ (resp. the nominal maximal density $\rho_{max} = 160\ veh/km$) times the number of lanes on the branch. The maximal flow (or capacity) $f^\alpha_{max}$ is given by $v^\alpha_{max}\rho^\alpha_c$ where $v^\alpha_{max}$ is the maximal speed on branch $\alpha$.

The Hamiltonians $H^\alpha$ are defined in (20) according to the flow function $f^\alpha$. See also Remark 2 on weaker assumptions than (A1) on the Hamiltonians. We consider branches of length $L = 200\ m$ and we have $N_b := \left\lfloor \dfrac{L}{\Delta x} \right\rfloor$ points on each branch such that $i \in \{0, ..., N_b\}$.

### 4.2. Initial and boundary conditions.

**Initial conditions.** In traffic flow simulations it is classical to consider Riemann problems for the vehicles densities $(\rho^\alpha_0)$ at the junction point. We then consider

initial conditions $(u_0^\alpha(x))_{\alpha=1,\dots,N}$ corresponding to the primitive of the densities according to (25). We also take the initial label at the junction point such that

$$u_0^\alpha(0) =: u_0(0) = 0, \quad \text{for any} \quad \alpha.$$

We can check that if the initial densities $(\rho_0^\alpha)$ are piecewise constant, then the initial data $(u_0^\alpha(x))_{\alpha=1,\dots,N}$ satisfy (A0).

We are interested in the time evolution of the densities. We stop to compute once we get a stationary final state.

**Boundary conditions.** For any $i \leq N_b$ we use the numerical scheme (10) for computing $(U_i^{\alpha,n})$. Nevertheless at the last grid point $i = N_b$, we have

$$\frac{U_{N_b}^{\alpha,n+1} - U_{N_b}^{\alpha,n}}{\Delta t} + \max\left\{H_\alpha^+(p_{N_b,-}^{\alpha,n}), H_\alpha^-(p_{N_b,+}^{\alpha,n})\right\} = 0, \quad \text{for} \quad \alpha = 1,\dots,N,$$

where $p_{N_b,-}^{\alpha,n}$ is defined in (8) and we set the boundary gradient as follows

$$p_{N_b,+}^{\alpha,n} = \begin{cases} \dfrac{\rho_0^\alpha}{\gamma^\alpha}, & \text{if} \quad \alpha \leq N_I, \\ p_{N_b,-}^{\alpha,n}, & \text{if} \quad \alpha \geq N_I + 1. \end{cases}$$

These boundary conditions are motivated by our traffic application. Indeed while they are presented for the scheme (10) on $(U_i^{\alpha,n})$, the boundary conditions are easily translatable to the scheme (23) for the densities. For incoming roads, the flow that can enter the branch is given by the minimum between the supply of the first cell and the demand of the virtual previous cell which correspond to the value of $f$ evaluated for the initial density on the branch $\rho_0^\alpha$ (see Table 1). For outgoing roads, the flow that can exit the branch is given by the minimum between the demand of the last cell and the supply of the virtual next cell which is the same than the supply of the last cell.

**Remark 8.** From [27], we recall that to prescribe some supply/demand conditions at the boundaries of a branch is strictly equivalent to respect Bardos-LeRoux-Nédélec conditions [1].

4.3. **Simulation results for a diverge.** We consider the case of a *diverge*: one incoming road denoted $\alpha = 1$ dividing into two outgoing roads respectively denoted 2 and 3 (see Figure 8). This case could illustrate the case of an off-ramp on a beltway. We introduce $\gamma^\alpha$ which represents the proportion of vehicles which exit the junction point on the branch indexed by $\alpha$, with $\alpha = 2, 3$. These coefficients $\gamma^2$ and $\gamma^3$ are defined such as:

$$\gamma^2 + \gamma^3 = 1 \quad \text{and} \quad 0 \leq \gamma^2, \gamma^3 \leq 1.$$

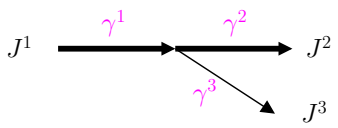


FIGURE 8. Diverge junction model

For the simulation, let us consider that roads 1 and 2 have both two lanes and that the maximal speed on both roads is supposed to be $v_{max}^{\{1,2\}} = 90$ km/h. Roads 1 and 2 represent the main section of the beltway. Road 3, corresponding to the

off-ramp, has a single lane and its maximal speed is $v^3_{max} = 50$ km/h. We assume that 80 percent of the vehicles coming from road 1 wish to continue on the main section while the remaining 20 percent exit the beltway. These values are recalled in Table 1.

| Branch | Number of lanes | Maximal speed (km/h) | $\gamma^\alpha$ |
|---|---|---|---|
| 1 | 2 | 90 | 1 |
| 2 | 2 | 90 | 0.80 |
| 3 | 1 | 50 | 0.20 |

TABLE 1. Traffic flow characteristics of each branch

We then consider the flow functions $f^\alpha$ according to the values of Table 1 (see Figure 9). The values of densities and flows for initial and final states are summarized in Table 2. They are respectively plotted on (a) and (d) of Figure 12.

| | Initial state | | Final state | |
|---|---|---|---|---|
| Branch | Density (veh/km) | Flow (veh/h) | Density (veh/km) | Flow (veh/h) |
| 1 | 50 | *3533* | 40 | *3600* |
| 2 | 20 | *2250* | 28 | *2880* |
| 3 | 30 | *962* | 12 | *720* |

TABLE 2. Values of densities and flows for initial and final states on each branch

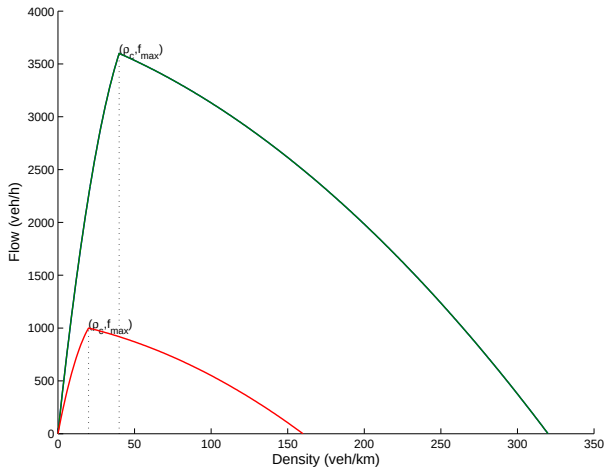


FIGURE 9. Graphs of the functions $f^\alpha$

**Vehicles labels and trajectories.** Hereafter we consider $\Delta x = 5m$ (that corresponds to the average size of a vehicle) and $\Delta t = 0.16s$.

The numerical solution $(U_i^{\alpha,n})$ is depicted on Figure 10. The vehicles trajectories are deduced by considering the iso-values of the labels surface $(U_i^{\alpha,n})$ (see Figure 11). In this case, one can observe that the congestion (described in the next part) induces a break in the velocities of the vehicles when going through the shock waves. It is still true through the junction point.

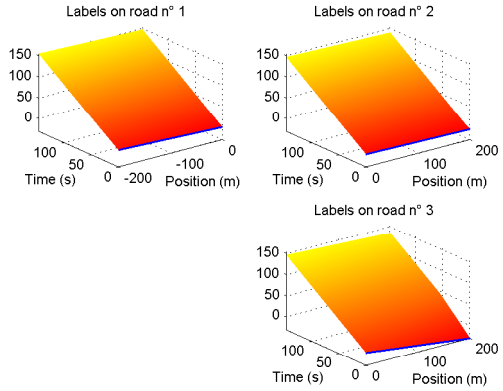


FIGURE 10. Numerical solution on each branch for the diverge

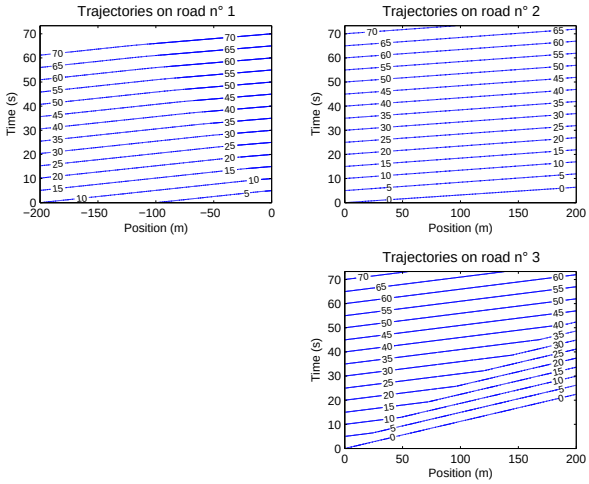


FIGURE 11. Trajectories of some vehicles on each branch for the diverge

**Propagation of waves.** Let us describe in detail the shock and rarefaction waves that appear from the considered initial Riemann problem (see Figure 12). We first notice that at the initial time, roads 1 and 3 are congested (see Figure 12 (a)). The incoming road has a demand of $3600veh/h$ splitted into $2880veh/h$ toward road 2 and $720veh/h$ toward road 3. The supplies on roads 2 and 3 are respectively $3600veh/h$ and $962veh/h$. Thus the partial demands are totally satisfied on both outgoing roads. On road 1 (see the Figure 12 (b) and (c)), the vehicles density

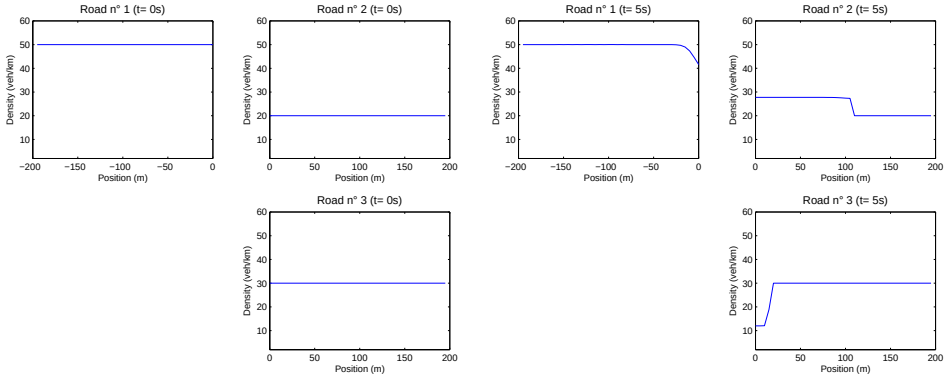


(a) Initial conditions for densities

(b) Densities at $t = 5$ s

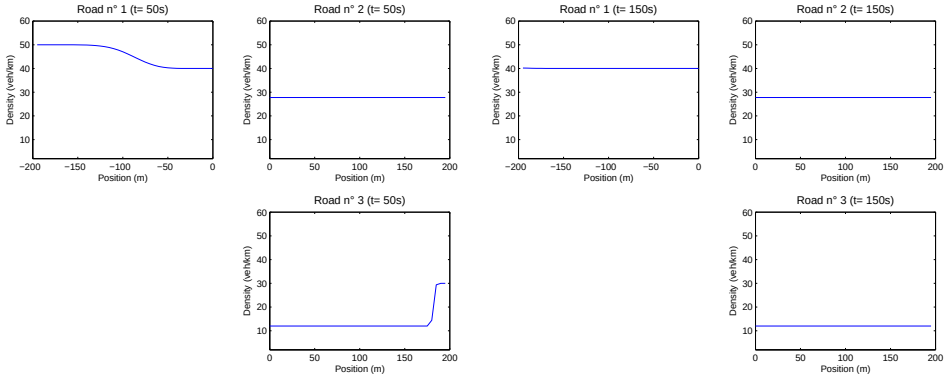


(c) Densities at $t = 50$ s

(d) Densities at $t = 150$ s

FIGURE 12. Time evolution of vehicles densities on a diverge

decreases from $50veh/km$ to the critical density $40veh/km$ and thus the flow increases to $3600veh/h$. There is the apparition of a rarefaction wave which should propagate at the speed given by the Rankine-Hugoniot formula

$$v^1 = \frac{[f^1]}{[\rho^1]} = \frac{3533 - 3600}{50 - 40} = -6.7 \text{ km/h}.$$

The negative sign means that the rarefaction wave propagates backward. Road 3 is no longer congested because the demand is fully satisfied and the vehicles can go freely on the branch (see the Figure 12 (b) and (c)). The flow goes from $962veh/h$ to $720veh/h$ and the density collapses from $30veh/km$ to $12veh/km$. Then a shock wave propagates forward at the speed $v^3 = 13km/h$ which matches to the Rankine-Hugoniot speed. On road 2, a rarefaction wave appears and propagates at speed $v^2 = 79km/h$ which matches to the Rankine-Hugoniot speed. The flow increases from $2250veh/h$ to $2880veh/h$ and the density goes from $20veh/km$ to $28veh/km$ (see the Figure 12 (b) and (c)).

4.4. **Simulation results for a merge.** We consider the case of a *merge*: two incoming roads denoted $\alpha = 1$ and 2 merging into a single outgoing road denoted 3 (see Figure 13). This case could illustrate the case of an on-ramp on a beltway.

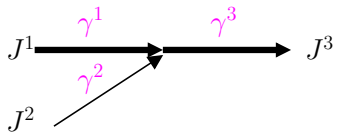


FIGURE 13. Merge model

For the numerical simulation, let us consider the characteristics summarized in Table 3. We assume that 80 percent of the through-flow comes from road 1 while the remaining 20 percent comes from the on-ramp 2.

**Remark 9.** Notice that for $N_I \geq 2$ incoming roads, a realistic choice of coefficients $(\gamma^\alpha)_{\alpha=1,\dots,N}$ is not obvious. We discuss that point in Section 5. Here we assume that the mix coefficients $(\gamma^\alpha)_{\alpha\leq N_I}$ are capacity proportional that is the ratio of the maximal flows that each incoming road could send to the junction point. This choice is motivated by what it was already established by empirical data sets in [2, 6] for which the merge ratios were closely related to the number of lanes per incoming branches.

| Branch | Number of lanes | Maximal speed (km/h) | $\gamma^\alpha$ |
|---|---|---|---|
| 1 | 3 | 90 | 0.80 |
| 2 | 1 | 70 | 0.20 |
| 3 | 3 | 90 | 1 |

TABLE 3. Traffic flow characteristics of each branch

We then consider the flow functions $f^\alpha$ according to the values of Table 3 (see Figure 14). The values of densities and flows for initial and final states are summarized in Table 4. They are respectively plotted on (a) and (d) of Figure 18.

| | Initial state | | Final state | |
|---|---|---|---|---|
| Branch | Density (veh/km) | Flow (veh/h) | Density (veh/km) | Flow (veh/h) |
| 1 | 50 | *4875* | 189 | *4320* |
| 2 | 20 | *1400* | 68 | *1080* |
| 3 | 30 | *3375* | 60 | *5400* |

TABLE 4. Values of densities and flows for initial and final states on each branch

**Vehicles labels and trajectories.** Hereafter we consider $\Delta x = 5m$ (that corresponds to the average size of a vehicle) and $\Delta t = 0.09s$.

The numerical solution $(U_i^{\alpha,n})$ is depicted on Figure 15. The vehicles trajectories are deduced by considering the iso-values of the labels surface $(U_i^{\alpha,n})$ (see Figure 16).

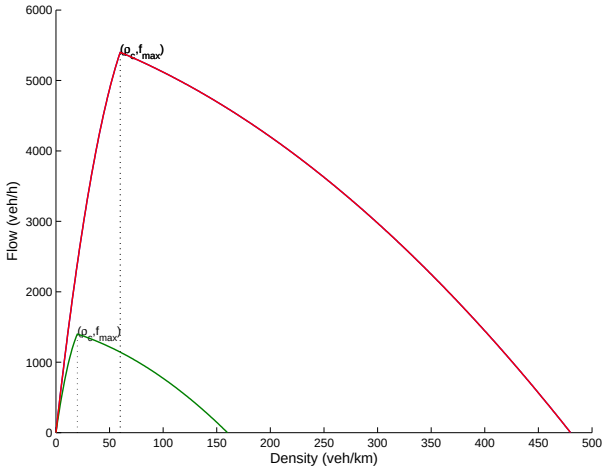


FIGURE 14. Graphs of the functions $f^\alpha$

Once again, we can notice that the congestion spillback (described in the next part) induces a break in the velocity of the vehicles when going through the shock waves. It is still true through the junction point.

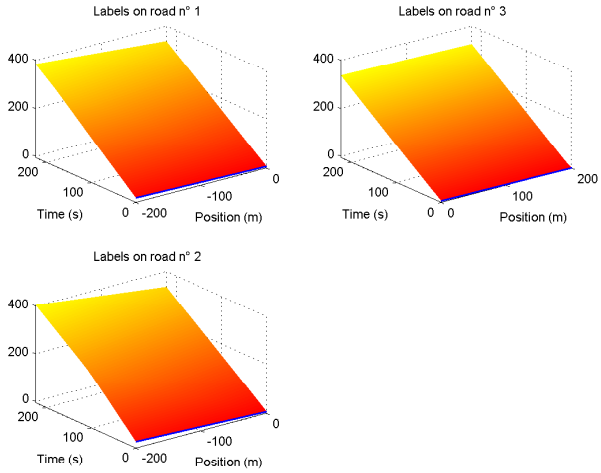


FIGURE 15. Numerical solution on each branch for the merge

**Propagation of waves.** Let us describe in detail the shock and rarefaction waves that appear from the considered initial Riemann problem (see Figure 18). At the initial state (see Figure 18 (a)) all the branches are not congested. At the initial state the supply on road 3 is $5400veh/h$ while the demands on roads 1 and 2 are respectively $4900veh/h$ and $1400veh/h$, that to say a total demand of $6300veh/h$. Thus all the demand can not be satisfied through the junction point. The junction is thus supply constrained and the flows are regulated by a priority share between both competitive roads.

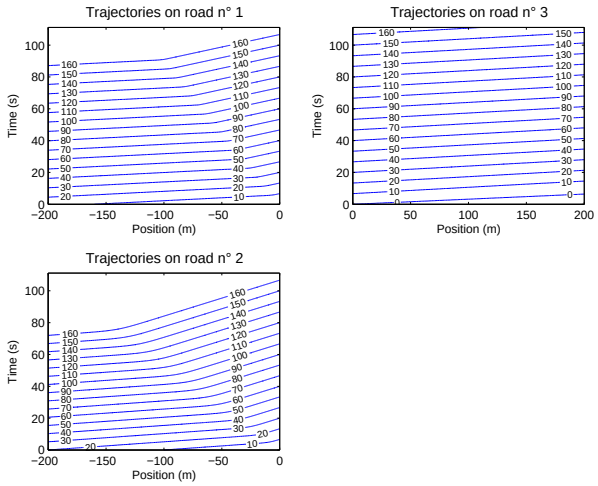


FIGURE 16. Trajectories of some vehicles on each branch for the merge

To understand the behaviour of the flows at the junction point, we adopt the optimization viewpoint (see Figure 17). The share is given by the fixed mix coefficients $\gamma^\alpha$ with $\alpha = \{1, 2\}$. The supply of road 3 is divided into roads 1 and 2 such that $f_S^{\{1\to 3\}} = 0.8 f_S^3$ and $f_S^{\{2\to 3\}} = 0.2 f_S^3$ that is $f_S^{\{1\to 3\}} = 4320 veh/h$ and $f_S^{\{2\to 3\}} = 1080 veh/h$.

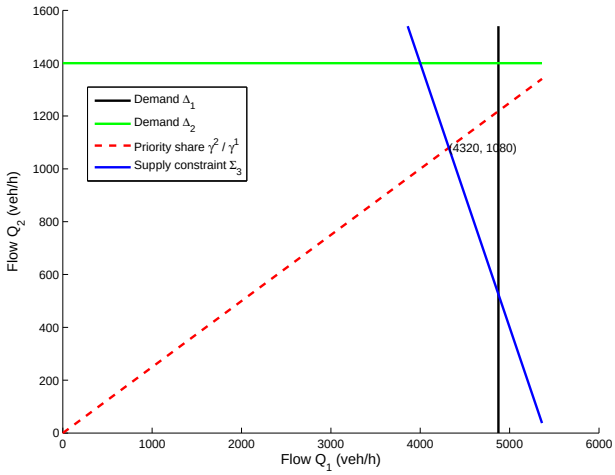


FIGURE 17. Flows distribution at merge

The flow through the junction is limited by the supply and it is weaker than the demands on both incoming roads (see Figure 17). Then there are shock waves that propagate backward on each incoming road (see Figure 18 (b) and (c)). The waves speeds should match the Rankine-Hugoniot speeds, that is $-4 km/h$ on road 1 and

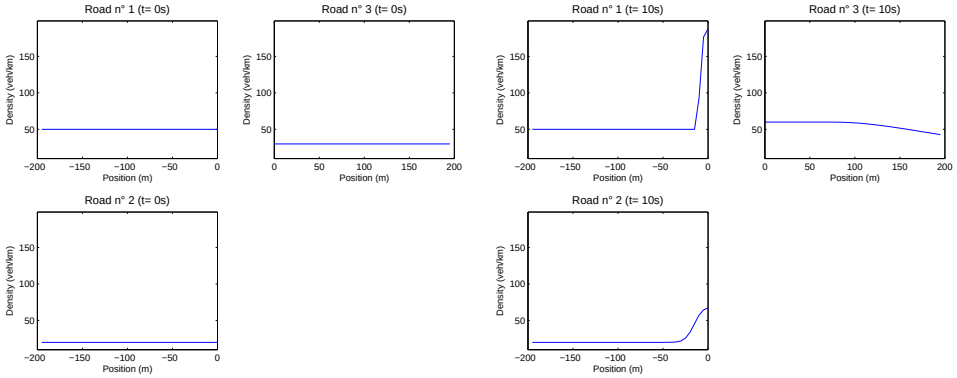


(a) Initial conditions for densities

(b) Densities at $t = 10$ s

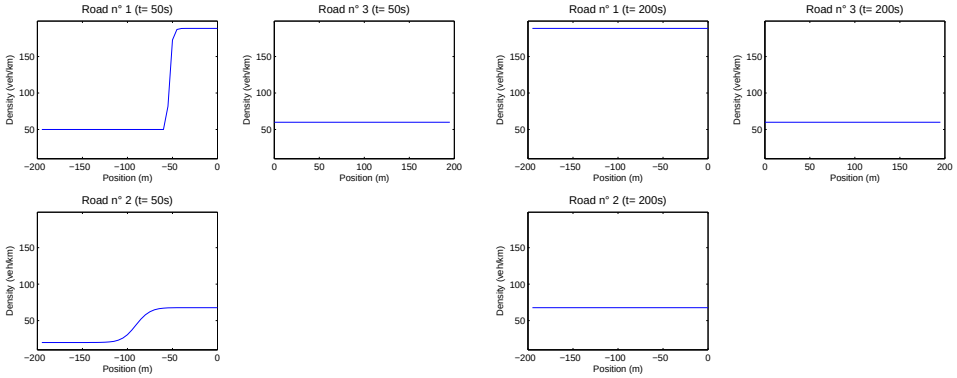


(c) Densities at $t = 50$ s

(d) Densities at $t = 200$ s

FIGURE 18. Time evolution of vehicles densities on a merge

$-7km/h$ on road 2. Moreover a rarefaction wave appears on the outgoing road 3 and it propagates at the same speed than the traffic flow (see Figure 18 (b)). The flux on road 3 reaches the capacity.

5. **Extensions.** We discuss hereafter some possible extensions for the model (1)-(2) and the numerical scheme (10)-(11). We recall that our numerical scheme allows to find an approximate solution which converges to the exact solution of (1)-(2) when the time and space steps go to zero. However, we can improve the realism of the HJ model by considering a more general law (even sub optimal) for the junction condition or to numerically deal with time dependent coefficients $\gamma^{\alpha}(t)$.

**Junction condition.** Up to now, we have only considered the maximization of the total amount of incoming flows in the perspective of a system optimum. However it is classical to observe that the passing flow through the junction is often (if not always) sub-optimal. It is particularly the case when the number of incoming branches is strictly greater than 1, due to competitive aspects of the merging. That is the reason why it should be interesting to consider another condition $F$ which is less than the function $F_0$ (the maximal theoretical flow that could pass through the

junction) given by

$$F_0(\gamma) := \min\left\{ \min_{\beta \le N_I} \frac{1}{\gamma^\beta} f_D^\beta(\rho_{-1}^{\beta,n}),\ \min_{\lambda \ge N_I+1} \frac{1}{\gamma^\lambda} f_S^\lambda(\rho_0^{\lambda,n}) \right\}. \tag{30}$$

The condition $F \le F_0$ could be obtained by considering a simple penalization of the optimal flow according to the load of competitive flows at the junction. The very recent paper [20] extends the mathematical results of [21] to more general junction conditions considering a flux limiter. The uniqueness of the solution to HJ equations still holds.

**Fixed coefficients.** The reader can notice that the flux coefficients $\gamma^\alpha$ for any $\alpha = 1, ..., n+m$ are already considered known at the beginning of the simulations. Moreover we suppose that these coefficients are given constant during the whole duration of the simulations. Both assumptions are not so realistic in a strict traffic context. Indeed for the incoming roads, the coefficients $\gamma^\alpha$ could be interpreted as *mixing coefficients* of the incoming flows through the junction point. For instance, consider a junction with two incoming roads for which the *mixing* coefficients depend on time and on the state of traffic. If the coefficients are chosen such that the road with the higher flow has the weakest mixing coefficient, then the main flow will be restricted in the junction model. In reality, the mixing coefficients are time dependent. It is obvious in the case of a signalized junction with priority rules or stop lights management. Fixed coefficients are only justified for a stationary traffic flow.

**Numerical extension for non-fixed coefficients** $(\gamma^\alpha)$**.** Up to now, we were considering fixed coefficients $\gamma := (\gamma^\alpha)_\alpha$ and the flux of the scheme at the junction point at time step $n \ge 0$ was (30).

In certain situations, we want to maximize the flux $F_0(\gamma)$ for $\gamma$ belonging to an admissible set $\Gamma$. Indeed we can consider the set

$$A := \operatorname*{argmax}_{\gamma \in \Gamma} F_0(\gamma).$$

In the case where this set is not a singleton, we can also use a priority rule to select a single element $\gamma^{*,n}$ of $A$. This defines a map

$$\left( (\rho_{-1}^{\beta,n})_{\beta \le N_I}, (\rho_0^{\lambda,n})_{\lambda \ge N_I+1} \right) \mapsto \gamma^{*,n}.$$

At each time step $n \ge 0$ we can then choose this value $\gamma = \gamma^{*,n}$ in the numerical scheme (23)-(24).

**Towards a new model for non-fixed coefficients?** Both previous parts about junction condition and fixed coefficients point out some rigidity of the framework given by the model (1). This model is particularly convenient to treat the flows on a junction in a unified approach, i.e. without considering incoming or outgoing roads. However it has the drawback of introducing fixed coefficients $(\gamma^\alpha)$ which are hard to use in traffic modelling.

As a first extension, we can introduce non-fixed coefficients for the traffic flow model (15), (26). However, the vehicles labels $u^\alpha$ are defined in (17) according to the vehicles densities $\rho^\alpha$ and up to the coefficients $\gamma^\alpha$. It is not obvious that in this case (with non-fixed coefficients $\gamma^\alpha(t)$), the vehicles labels still satisfy the model (1).

Another extension could be to introduce assignment coefficients $\gamma_{ij}$ which stand for the percentage of vehicles coming from branch $i$ and going on branch $j$. It is not suitable with the model (1) even if we sort incoming and outgoing branches.

**Remark 10.** In traffic flow litterature, [5] already introduces junction models with dependent coefficients $\gamma^\alpha(\rho)$. However the developed methods are no longer satisfactory because these models do not comply the invariance principle of [27].

6. **Conclusion.** In this article, we provide a discussion about traffic flow modelling on junctions. Using the well-known links between scalar conservation laws and Hamilton-Jacobi equations of the first order on a simple section, a new framework has been built to model junctions [20, 21]. This framework based on Hamilton-Jacobi equations allows to overpass certain shortcuts of the classical approach [13], yielding e.g. the uniqueness of the solution whatever the number of incoming or outgoing branches. Thus we can built a numerical scheme that converges to that unique solution. The mathematical properties of the numerical scheme are deeply investigated in a companion article [10].

The numerical scheme we propose for Hamilton-Jacobi equations is strictly equivalent to the Godunov scheme for conservations laws. The numerical tests performed in this paper attempt to illustrate the ability of the scheme to reproduce kinematic waves such as shocks or rarefaction fans. For a deeper numerical comparison between numerical schemes (in the conservation laws framework), the interested reader is referred to [3, 4]. It is out of the scope here.

**Aknowledgements.** The authors are grateful to Prof. R. Monneau for many valuable comments on the organization of the paper. We also would like to thank the anonymous reviewers and all the organizers of TRAM2 workshop, namely Profs. Bayen, Colombo, Goatin and Piccoli. This work was partially supported by the ANR (Agence Nationale de la Recherche) through HJnet project ANR-12-BS01-0008-01.

## REFERENCES

[1] C. Bardos, A. Y. Le Roux, and J.-C. Nédélec, *First order quasilinear equations with boundary conditions*, Comm. Partial Differential Equations, 4 (1979), pp. 1017-1034.
[2] H. Bar-Gera, S. Ahn, *Empirical macroscopic evaluation of freeway merge-ratios*, Transport. Res. C 18 (2010), pp. 457-470.
[3] G. Bretti, R. Natalini and B. Piccoli, *Fast algorithms for the approximation of a fluid-dynamic model on networks*, Discrete Contin. Dyn. Syst. Ser. B, 6 (2006), pp. 427-448.
[4] G. Bretti, R. Natalini and B. Piccoli, *Numerical approximations of a traffic flow model on networks*, Networks and Heterogeneous Media, 1 (2006), pp. 57-84.
[5] C. Buisson, J.P. Lebacque, and J.B. Lesort, *STRADA: A discretized macroscopic model of vehicular traffic flow in complex networks based on the Godunov scheme*, In: Proceedings of the IEEE-SMC IMACS'96 Multiconference, Symposium on Modelling, Analysis and Simulation Vol 2 (1996), pp. 976-981.
[6] M.J. Cassidy and S. Ahn, *Driver turn-taking behavior in congested freeway merges*, Transportation Research Record, Journal of the Transportation Research Board 1934 (2005), pp. 140-147.
[7] C. Claudel and A. Bayen, *Lax-Hopf based incorporation of internal boundary conditions into Hamilton-Jacobi equation. Part I: Theory*, IEEE Transactions on Automatic Control. 55(5), (2010), pp. 1142-1157.
[8] G. M. Coclite, M. Garavello, and B. Piccoli, *Traffic Flow on a Road Network*, SIAM J. Math. Anal. 36 (no. 6), (2005), pp. 1862-1886.
[9] R. Corthout, G. Flötteröd, F. Viti and C.M.J. Tampère, *Non-unique flows in macroscopic first-order intersection models*, Transport. Res. B 46 (2012) pp. 343-359.
[10] G. Costeseque, J-P. Lebacque and R. Monneau, *A convergent scheme for Hamilton-Jacobi equations on a junction: application to traffic*, submitted (2013).
[11] C.F. Daganzo, *On the variational theory of traffic flow: well-posedness, duality and applications*, Networks and Heterogeneous Media, AIMS, vol.1, n4, December 2006, pp. 601-619.

[12] G. Flötteröd and J. Rohde, *Operational macroscopic modeling of complex urban intersections*, Transport. Res. B, 45 (2011), pp. 903-922.
[13] M. Garavello and B. Piccoli, *Traffic flow on networks*, vol.1 of AIMS Series on Applied Mathematics, American Institute of Mathematical Sciences (AIMS), Springfield, MO, 2006.
[14] N.H. Gartner, C.J. Messer and A.K. Rathi, *Revised Monograph of Traffic Flow Theory*, Online publication of the Transportation Research Board, FHWA, (2001), http://www.tfhrc.gov/its/tft/tft.htm.
[15] J. Gibb, *A model of traffic flow capacity constraint through nodes for dynamic network loading with queue spillback*, Transportation Research Record: Journal of the Transportation Research Board (2011), pp. 113-122.
[16] S.K. Godunov, *A finite difference method for the numerical computation of discontinuous solutions of the equations of fluid dynamics*, Math. Sb., 47 (1959), pp. 271-290.
[17] S. Göttlich, M. Herty, U. Ziegler, *Numerical Discretization of Hamilton-Jacobi Equations on Networks*, Networks and Heterogeneous Media, 8 (2013), pp. 685-705.
[18] K. Han, B. Piccoli, T.L. Friesz, T. Yao, *A continuous-time link-based kinematic wave model for dynamic traffic networks*, arXiv preprint arXiv:1208.5141, (2012).
[19] H. Holden and N. Risebro, *A mathematical model of traffic flow on a network of unidirectional roads*, SIAM J. Math. Anal. 4, (1995), pp. 999-1017.
[20] C. Imbert and R. Monneau, *The vertex test function for Hamilton-Jacobi equations on networks*, arXiv preprint arXiv:1306.2428 (2013).
[21] C. Imbert, R. Monneau and H. Zidani, *A Hamilton-Jacobi approach to junction problems and application to traffic flows*, ESAIM Control Optim. Calc. Var., 19 (2013), pp. 129-166.
[22] M.M. Khoshyaran and J.P. Lebacque, *Internal state models for intersections in macroscopic traffic flow models*, accepted in Proceedings of Traffic and Granular Flow09, (2009).
[23] J.A. Laval, L. Leclercq, *The Hamilton-Jacobi partial differential equation and the three representations of traffic flow*, Transport. Res. B 52 (2013), pp. 17-30.
[24] J.P. Lebacque, *Semi-macroscopic simulation of urban traffic*, Proc. of the Int. 84 Minneapolis Summer Conference. AMSE 4 (1984), pp. 273-291.
[25] J.P. Lebacque, *The Godunov scheme and what it means for first order traffic flow models*, In J. B. Lesort, editor, 13th ISTTT Symposium, Elsevier, New York, 1996, pp. 647-678.
[26] J.P. Lebacque and M.M. Khoshyaran, *Macroscopic flow models ( First order macroscopic traffic flow models for networks in the context of dynamic assignment)*, In M. Patriksson et M. Labbé eds., Transportation planning, the state of the art, Klwer Academic Press, 2002, pp. 119-140.
[27] J.P. Lebacque and M.M. Koshyaran, *First-order macroscopic traffic flow models: intersection modeling, network modeling*, In H.S. Mahmassani, editor, Proceedings of the 16th International Symposium on the Transportation and Traffic Theory, College Park, Maryland, USA, Elsevier, Oxford, 2005, pp. 365-386.
[28] M. J. Lighthill and G. B. Whitham, *On kinetic waves. II. Theory of Traffic Flows on Long Crowded Roads*, Proc. Roy. Soc. London Ser. A, 229 (1955), pp. 317-345.
[29] G.F. Newell, *A simplified theory of kinematic waves in highway traffic, (i) General theory, (ii) Queueing at freeway bottlenecks, (iii) Multi-destination flows*, Transport. Res. B 4 (1993), pp. 281-313.
[30] P. I. Richards, *Shock Waves on the Highway*, Oper. Res., 4 (1956), pp. 42-51.
[31] C. Tampere, R. Corthout, D. Cattrysse and L. Immers, *A generic class of first order node models for dynamic macroscopic simulations of traffic flows*, Transport. Res. B, 45 (2011), pp. 289-309.

*E-mail address*: costeseg@cermics.enpc.fr
*E-mail address*: jean-patrick.lebacque@ifsttar.fr